Radiation defects in ion-implanted silicon. I. Mössbauer spectroscopy of ^{119}Sn defect structures from implantations of radioactive antimony

G. Weyer, A. Nylandsted Larsen,* N. E. Holm, and H. L. Nielsen
Institute of Physics, University of Aarhus, DK-8000 Aarhus C, Denmark
(Received 31 January 1979)

Impurity-defect structures in silicon containing ^{119}Sn have been studied by Mössbauer spectroscopy. The defects have been created by isotope-separator implantation of radioactive $^{119}Sb^+$ ions at room temperature. Emission spectra of the 24-keV Mössbauer γ radiation from the daughter ^{119}Sn have been measured. The Mössbauer spectra are analyzed in terms of four independent lines. These lines are characterized by the measured isomer shifts, linewidths, quadrupole splittings, and Debye-Waller factors. From these parameters, different bonding configurations are deduced for the Sn impurity atoms. Thus, the lines are assigned to emitting Sn atoms as substitutional impurities and as atoms in more complex impurity-defect structures. The formation of the impurity-defect structures in the implantation process (and their annealing behavior) is controlled by properties of the antimony atoms, whereas the measured Mössbauer parameters reflect the response of the Sn daughter atoms in these structures. It is concluded that a large fraction of the Sn atoms occupy locally undisturbed, substitutional lattice sites [with an isomer shift of $\delta = 1.83(6)$ mm/s and a Debye temperature of $\Theta = 220(20)$ K]. A minor fraction is in interstitial lattice positions [$\delta = 3.3(1)$ mm/s, $\Theta = 240(30)$ K]. Two other lines [$\delta = 2.6(1)$ mm/s, $\Delta E_Q \approx 0.3$ mm/s, $\Theta = 160(20)$ K, and $\delta \approx 2.6$ mm/s, $\Theta = 250(40)$ K] are attributed to vacancy associated Sn impurity atoms. Rough annealing experiments show annealing of the Sb impurity vacancy complex (with $\Theta = 160$ K) between 700 and 900 K. The other impurity-vacancy structure ($\Theta = 250$ K) is only formed after high-temperature treatment of the sample ($\gtrsim 1200$ K). The interstitial fraction increases with annealing temperature.

I. INTRODUCTION

Ion-implantation techniques by means of mass separators have been utilized as a doping method in semiconductor technology in recent years. This method offers several advantages compared to conventional diffusion techniques for many requirements and has led to the development of new electronic components (see, e.g., Refs. 1 and 2). It is, however, a particular drawback of this method that undesired properties of the final product, e.g., a low fraction of electrically active impurity atoms, often result because of the radiation damage produced during the ion-implantation process. From the point of view of applications, the nature of this damage is not sufficiently known yet to either completely avoid its influence or possibly to make use of it. On the other hand, studies of radiation-damage structures can contribute to a fundamental understanding of the interactions in solids in an extreme nonequilibrium state created by the implantation of high-energy impurity atoms.

The mechanisms of the production of radiation damage in silicon by low-energy, heavy ions can be conveniently divided into three stages[3]:

In the first stage, host atoms are displaced from their lattice positions due to the transfer of energy by the incoming ions. The interactions determining the slowing-down process of the incoming ions have been investigated intensely, the range and distribution of the implanted ions are relatively well known (see, e.g., Ref. 4).

In stage two, simple defects (vacancy-interstitial pairs) are formed due to the displacement of the host atoms. The properties of these defects are determined by the energy transferred to the host atoms. Since the transferred energy in heavy-ion implantations is generally much larger than the minimum energy for the displacement of a host atom, the first struck atom can subsequently displace other atoms. A displacement cascade will result in which complex defects can be formed. Finally a region with a high defect concentration (disordered region) will be created. The formation of complex defects at this stage is assumed to be temperature independent. The dimensions and properties of the disordered region depend primarily on the ion-host atomic mass ratio and the energy of the incoming ion. Calculations of the distribution of radiation damage for Sb in silicon[5] taking multiple-collision cascades into account show a good

overall agreement with experimental results.[6] Recently, direct evidence for spike phenomena in heavy-ion implantations of silicon and germanium has been given (see Refs. 7 and references cited therein). However, the knowledge about the microscopic nature of the disordered region and the phenomenology of its defects is still relatively poor.

In the third stage the defects thus produced interact with each other and with impurity atoms. More complex defects are formed. The interactions and the formation of these defects are temperature dependent. Since defects are stable only below a characteristic temperature, for a given implantation or annealing temperature, primary defect structures can anneal and more complex defects can agglomerate. In such processes, the high density of defects in the disordered regions may be crucial for the formation of defect structures that are not produced by electron (or neutron) irradiation. Additionally, the ionization accompanying the implantation process might influence the annealing or formation of defects, since the mobility and stability of the defects will generally be charge-state dependent. Various aspects of ion-implantation radiation damage have been studied by a number of different experimental methods (for recent reviews, see Ref. 8).

The interactions in both stages two and three are presumably those determining the formation of defects containing the implanted impurity atoms. In particular, for room-temperature implantations in silicon as undertaken in this investigation, temperature-dependent interactions (stage 3) will be important as simple defects are known to be mobile at this temperature. For example, the trapping of simple defects at the impurity atoms is favored by certain properties of the impurity atoms (e.g., electrical charge). The defect types formed in such a way at the end of the track of the implanted atoms will depend critically on the "chemistry" of the impurities.

This paper deals with impurity-defect structures formed by implanted Sb atoms. These structures are studied in the following way: Radioactive ^{119}Sb atoms are implanted; they decay to an excited state of ^{119}Sn, which decays to the ground state by emission of a Mössbauer γ quantum. Mössbauer spectra of this emitted radiation give information on interactions of the Sn atoms in various daughter defect structures related to the parent defects formed by the Sb implantations. Thus it is possible to study defects containing Sn impurities which are not formed when Sn itself is implanted. In addition, from the ^{119}Sn Mössbauer spectra, information on some properties of the Sb defects can be obtained, e.g., the annealing properties. It is important to emphasize the dual origin of the Mössbauer spectrum of the impurity-containing defects: The configurational structure of the impurity defect is governed by the "chemistry" of Sb. This structure is sometimes, but not always, inherited by the Sn atom formed following the nuclear decay. The atomic, electronic structure determining the Mössbauer parameters is always that of the element Sn.

The electronic configuration of the Sn impurity atoms in the various defects can be deduced from the measured isomer shifts and quadrupole interactions. The bonding of the impurity atoms and their coupling to the host lattice can be studied by determining the Debye-Waller factors and their temperature dependence. These Mössbauer parameters (hyperfine-structure parameters and f factors) are predominantly sensitive to nearest-neighbor interactions of the impurity atoms. Therefore, aspects of the microscopic nature of defects containing impurity atoms can be investigated. High sensitivity for low concentrations of impurities is achieved by implantation of radioactive source nuclei. (The principles of Mössbauer spectroscopy can be found in Ref. 9.)

Properties of ^{119}Sn impurity atoms in silicon have been studied quite extensively by Mössbauer spectroscopy.[10–15] Spectra of ion-implanted ^{119}Sn have been measured for different implantation conditions.[10,12] Large substitutional fractions have been found. The isomer shift determined for substitutionally implanted ^{119}Sn is in agreement with that from diffused ^{119}Sn.[11,13–15] Qualitatively different influences of radiation defects on substitutional ^{119}Sn impurity atoms have been concluded for neutron irradiations[14,15] and activations[15] and ion implantations,[10,12] respectively.

A few Mössbauer experiments on Sb impurity atoms in silicon have been reported so far. Teague *et al.*[16] studied the Mössbauer absorption of diffused ^{121}Sb isotopes in highly-doped material. Van Rossum *et al.*[17] implanted radioactive ^{125}Sb and observed the Mössbauer transition of ^{125}Te. Broadened lines have been found, interpreted to originate from substitutional Sb. Both experiments suffer from a large natural linewidth of these transitions. Experiments on ^{119}Sb implanted at 700 K and at room temperature utilizing the higher resolution of the ^{119}Sn Mössbauer transition have been reported from this laboratory.[18,19] (Although the radioactive decay chain ^{119m}Te $\rightarrow$ ^{119}Sb $\rightarrow$ ^{119}Sn offers interesting applications for Mössbauer emission spectroscopy on the 24-keV transition of ^{119}Sn, this source has to our knowledge been only used by Llabador[20] and recently by Ambe and Ambe.[21]) In the present paper, spectra of high accuracy have been obtained by a resonance counting technique which allows a more detailed analysis compared to those reported previously. Measurements have been performed at room temperature and at 77 K to determine Debye temperatures for the impurity atoms in different defects. Annealing studies have been undertaken to investigate roughly the binding energies or kinetics of the defect structures.

II. EXPERIMENTAL

To prepare the ^{119}Sb, the ^{119}Te isomers (4.7 d ^{119m}Te and 16 h ^{119g}Te) were produced by irradiating natural Sn metal with 20-MeV α particles from the cyclotron of the Niels Bohr Institute in Copenhagen. The Sn target was prepared by letting molten Sn solidify on a silver cooling plate. The irradiated Sn target was separated from the Ag plate by dissolving it in concentrated HCl. A black residue remains when the target dissolved. This residue carries the Te activity almost quantitatively. The Te was extracted from the residue with HNO_3 to which 2 mg Te carrier was added. After removal of HNO_3 by fuming with HCl, elemental Te was precipitated from 4 M HCl with SO_2 gas. The Te precipitation was repeated in order to reduce the contamination with Sn. The 38-h ^{119}Sb activity was allowed to grow in the purified Te. One mg Sb carrier was added, and elemental Sb was precipitated from a hot 2 M HCl solution by reduction with Fe foils. The Sb was filtered and mounted in the ion source of the isotope separator. Further milking of ^{119}Sb was performed after a new growth period.

Implantations of ^{119}Sb were carried out at an energy of 60 keV at room temperature with an electromagnetic isotope separator. Single crystals of *n*-type silicon were implanted. The crystals, cut perpendicular to a major axis, were tilted by $\sim 7°$ relative to the beam axis to avoid an implantation in a channeled direction. The crystal surfaces were highly polished and cleaned chemically before the implantation.

An upper limit on the implanted dose was obtained from the ion current of the separation. The dose rate was $\lesssim 10^9$ atoms/cm^{2}s for the mass number 119. From the radioactivity of the implanted crystals, the number of implanted ^{119}Sb atoms was determined to be $\lesssim 10^{11}$ atoms/cm^2. The total implanted dose for mass number 119 (mainly ^{119}Sn) were $\lesssim 10^{13}$ and $\approx 10^{14}$ atoms/cm^2 for two implanted samples, respectively.

Mössbauer spectra were measured with a conventional electromechanical drive system sychronized to a multichannel analyzer operated in the multiscaling mode. The γ rays emitted from the implanted sources were detected in a resonance detector of the parallel-plate avalanche counter type.[22] SnO_2 resonance absorber material (enriched to ~ 90 at. % in ^{119}Sn) was applied to allow for fast data acquisition. Annealing of implanted samples was performed in a dry nitrogen atmosphere for 20 min. Afterwards the samples cooled to room temperature in ~ 5 min.

III. EXPERIMENTAL RESULTS AND DATA TREATMENT

Figure 1 shows Mössbauer spectra measured at 77 K directly after the implantation of ^{119}Sb at room temperature (upper spectrum) and after annealing of the sample for 20 min at ~ 900 K (lower spectrum). The latter spectrum has been analyzed assuming two emission lines from the source and, as for all further spectra, the known quadrupole splitting of the SnO_2-absorber material ($\Delta = 0.54$ mm/s) has been taken into account. A least-squares fit to the lower spectrum yields a line at $\delta = 1.90$ mm/s with a linewidth of $\Gamma = 0.98$ mm/s (a typical Γ value for this SnO_2 resonance detector setup) and a broadened line ($\Gamma \sim 1.2$ mm/s) at $\delta \sim 3.3$ mm/s with a much lower intensity. In the fit shown in Fig. 1, the position and width of the latter line have been fixed to values obtained from spectra where this line had a larger intensity and where its parameters could be determined more accurately (see Table I, sample 2 annealed at 1173 K). The upper spectrum of Fig. 1 has been analyzed assuming two emission lines, one of them, being identical to the line at $\delta = 1.90$ mm/s found in the lower spectrum, was fixed in position and linewidth values in the fit. With these constraints the fit yielded a line at $\delta = 2.59$ mm/s with a linewidth of $\Gamma = 1.37$ mm/s, as shown in Fig. 1.

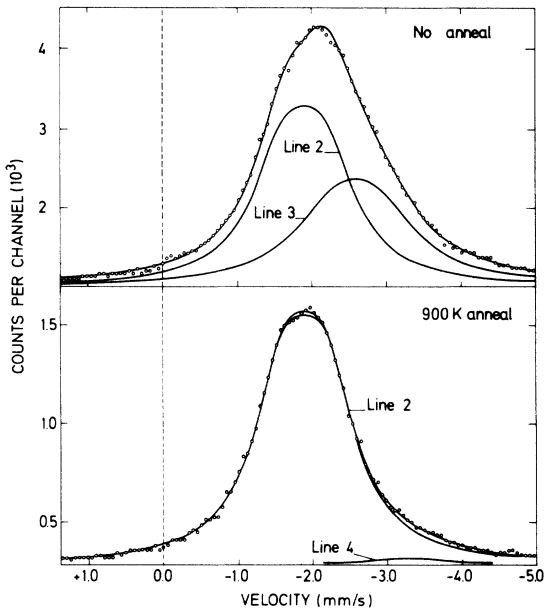

FIG. 1. Mössbauer spectra of ^{119}Sn in silicon from a room-temperature implantation of ^{119}Sb. The spectra have been measured at 77 K directly after the implantation (upper spectrum) and after an annealing of the sample at 873 K for 20 min (lower spectrum). The decomposition of the spectra into different lines and the curve obtained from a least-squares-fit procedure are shown by the drawn curves.

The results from a series of measurements on this implanted sample 2 at liquid nitrogen and room temperature after different high-temperature annealing treatments are listed in Table I. All spectra have been analyzed in terms of the above mentioned three

TABLE I. Results in chronological order from different postimplantation treatments of two samples of room-temperature-implanted ^{119}Sb in silicon single crystals (fz, n type, 5 Ω cm) where δ_i is the isomer shift relative to SnO_2, Γ_i the linewidth, I_i the relative intensity (arbitrary units), f_i the Debye-Waller factors at the relevant measuring temperatures, and P_i the I_i/f_i (arbitrary units).

Sample	Meas. temp. (K)	Sample treatment	Line 2 δ_2 (mm/s)	Line 2 Γ_2 (mm/s)	Line 2 I_2	Line 3 or 3′ δ_3 (mm/s)	Line 3 or 3′ Γ_3	Line 3 or 3′ I_3	f_3	f_3'	Line 4 δ_4 (mm/s)	Line 4 Γ_4 (mm/s)	Line 4 I_4	$\sum_i P_i$
	297	as impl.	1.83[a]	0.93[a]	0.76	2.63[a]	1.17	0.56	0.15	...				1.00
	77	as impl.	1.87[a]	0.93[a]	1.59	2.66	1.25	1.48	0.64	...				0.94
1	77	ann. 683 K	1.87[a]	0.93[a]	1.26	2.61	1.30	1.63	0.64	...				0.89
	77	ann. 873 K	1.87	0.93	3.53	...	...	...	...	...	3.30[a]	1.22	0.12	1.00
	77	ann. 1173 K	1.87[a]	0.93[a]	2.62	2.61[a]	1.30[a]	0.59	...	0.84	3.30	1.24	0.52	1.00
	77	as impl.	1.90[a]	0.98[a]	1.88	2.59	1.37	1.40	0.64	...	...	...	...	0.98
	77	ann. 873 K	1.90	0.98	3.83	...	...	...	...	...	3.29[a]	1.22[a]	0.10	1.06
	77	ann. 1173 K	1.90[a]	0.98[a]	3.59	...	...	...	...	...	3.32	1.12	0.30	1.06
2	297	ann. 1173 K	1.83	0.94	1.83	...	...	...	...	...	3.29[a]	1.22	0.06	1.02
	77	ann. 1373 K	1.90[a]	0.98[a]	2.37	2.70	0.83	0.45	...	0.84	3.32[a]	1.12[a]	0.97	1.02
	297	ann. 1373 K	1.83[a]	0.94[a]	1.29	2.61[a]	1.16[a]	0.30	...	0.51	3.32[a]	1.12[a]	0.33	1.00
	77	HNO_3 etch.	1.89	1.09	3.04	...	...	...	...	...	...	...	...	...

[a]Parameter fixed in the fit.

lines which have been labeled 2, 3, and 4 in the order of their isomer shifts. Spectra obtained after annealing at ~1200 K and ~1300 K measured at liquid nitrogen and at room temperature, respectively, are shown in Fig. 2. After an annealing at ~1200 K (spectrum a of Fig. 2), Sb is expected to start migrating. Line 4 is seen to increase but no qualitative changes of the spectrum are observed as compared to that after the 900 K annealing. Drastic changes are found after the annealing step at ~1400 K [spectrum 2(b)]. Besides a strong increase in the intensity of line 4, a line at $\delta \simeq 2.6$ mm/s, labeled line 3′, is found. This line has a relatively large intensity in the spectra, however, it is not shown in the analysis of Fig. 2(c).

Figure 2, spectrum 2(c), shows that it is possible to obtain a satisfactory fit to the room-temperature spectrum without the assumption of a line at $\delta \sim 2.6$ mm/s, i.e., with a fixed line at $\delta = 1.83$ mm/s and only one additional line. However, no consistent fit to both spectra from this sample measured at 77 [2(b)] and 297 K [2(c)] can be obtained if only two

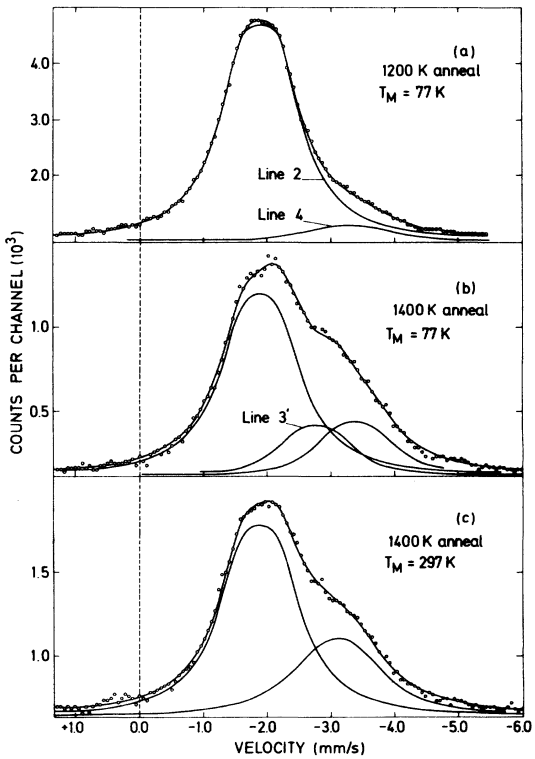

FIG. 2. Mössbauer spectra of ^{119}Sn in silicon from a room-temperature implantation of ^{119}Sb. The spectra have been measured after a subsequent annealing at 1173 K (a) and 1373 K (b) and (c). Spectra (a) and (b) are measured at 77 K and spectrum (c) at 279 K. Curves obtained from least-squares-fit procedures in terms of different lines are indicated. Spectra (b) and (c) have been analyzed assuming three and two lines to be present, respectively (see text).

lines are included. A comparison of spectrum 2(c) to spectrum 2(b) shows that one must add a third line at $\delta = 2.6$ mm/s. Both spectra are explained consistently with only three lines. In particular, the parameters for lines 2 and 4 remain the same as before the annealing at ~1400 K.

The results from similar experiments on a second implanted sample (sample 1) are included in Table I. Again an analysis in terms of three lines has been achieved by fixing the position of line 2 from the spectrum after an annealing at ~900 K. The results are in good agreement with those obtained for sample 2. The annealing temperature of line 3 is between ~700 and 900 K. For sample 1 already after the 1200 K annealing large intensities are found for lines 3′ and 4.

In order to find the origin of these two lines after the 1400 K treatment of sample 2, the implanted layer ($\lesssim$300 Å) was removed by firstly etching with boiling HNO_3 and subsequently treating the sample with HF. The spectrum measured after this procedure should then stem mainly from Sb diffused into the nonimplanted bulk material. The measured spectrum showed only an emission line at $\delta = 1.9$ mm/s. Thus lines 3′ and 4 originate from Sb in the implanted layer.

From the measurements at room temperature and at 77 K, the Debye temperature Θ for the individual lines can be obtained from a high-temperature Debye approximation for the Debye-Waller factor $f = \exp(-6E_R T/k\Theta^2)$.[9] Here E_R is the recoil energy of the emitting nucleus and k is Boltzmann's constant. Since the intensity of a line I_i is proportional to the relative fraction of emitting atoms associated with the specific defect i, p_i, and to the Debye-Waller factor f_i, the Debye temperature can be determined from the intensity ratio at two different temperatures. The Debye-Waller factors can then be calculated from the high-temperature approximation and the relative number of defects can be deduced. From the annealing experiments an independent test on the reliability of the assumption of individual lines and their Debye-Waller factors can be obtained from the normalization condition for all emitting atoms: $\sum_i p_i = \sum_i I_i f_i^{-1} = \text{const}$. These sums are included in Table I and it can be concluded that they are reasonably constant. The following average Debye temperatures are deduced: $\Theta_2 = 220(20)$ K, $\Theta_4 = 240(30)$ K, $\Theta_3 = 160(20)$ K before annealing at ~1200 K, $\Theta_3' = 250(40)$ K, after annealing at 1200 K. (A possible systematic error due to the application of the high-temperature approximation is $\lesssim|-3\%|$ and has not been included in the above values.) The changes in line positions due to the second-order Doppler shift are found to be roughly in accordance with the above Debye temperatures for lines 2 and 3. The average isomer shifts for the three lines are determined to be $\delta_2 = 1.83(6)$ mm/s, $\delta_3 = \delta_3' = 2.60(10)$ mm/s, and $\delta_4 = 3.30(10)$ mm/s at room temperature (uncorrected for a possible geometrical velocity error of $\lesssim|-0.04|$ mm/s).

IV. DISCUSSION

The analysis of all spectra from samples measured or annealed at different temperatures in terms of only four lines, is now considered sufficiently well established to serve as a basis for the interpretation of the experiments. The individual lines are defined by their isomer shifts (and quadrupole splittings) and are distinguished further by different Debye temperatures. Although the spectroscopic resolution in a single spectrum may be poor, their existence can be unambiguously concluded from the combination of all experimental results (cf. also Part II of this paper). These four lines originate from impurity atoms in different defects of the host lattice. The questions arise: What is the lattice location of the impurity atoms in these defects? What can be learned about the properties of these defects from the Mössbauer experiments? Finally, can a self-consistent interpretation of these and related experiments be given?

A. Considerations on the influence of the electron capture decay of the Mössbauer source nuclei on the measured spectra

In a discussion of the origin of the measured lines, the influence of the ^{119}Sb radioactive decay on the spectra measured for the 24-keV transition of ^{119}Sn has to be considered. Two effects of the nuclear decay may be important. Firstly, a displacement of the decaying impurity atom might occur due to the recoil energy transferred to the nucleus, and secondly, immediately after the electron-capture decay the Sn atoms will be left in nonequilibrium charge states. This may influence the structure of the final, detected defects.

The displacement energy of a substitutional silicon atom is about 20–25 eV.[23] This holds approximately for a substitutional Sb atom, too. However, a vacancy associated Sb atom is expected to possess a reduced displacement energy. An estimate based on force constants calculated from a Debye model by using the experimental Debye temperatures yields a reduction of the displacement energy of no more than 50% (see discussion in Secs. IV C and E). Since the recoil energy of the electron capture (EC) decay of ^{119}Sb is about 2 eV, no permanent displacement of the decaying atom is anticipated.

In the electron-capture decay of ^{119}Sb, a K electron will be captured with a high probability. Thus immediately after the nuclear decay the daughter ^{119}Sn atom will have a hole in the K shell. The lifetime for a K hole in the host material silicon has been es-

timated to be $\sim 1.5 \times 10^{-15}$ s.[24] The lifetime can be expected to be even shorter for the Sn atom.[25] The hole in the K shell will be removed by the emission of x rays or Auger electrons which in turn can create several holes in the outer electronic shells. As a net result the atom can be left in a highly charged state. These processes can be assumed to occur in times that are much shorter than the lifetime of the Mössbauer state ($\tau = 2.8 \times 10^{-8}$ s). The time for the refilling of the final holes in the valence shells in silicon has been estimated to be 4×10^{-17} s.[26] Thus it can be assumed that the decaying atoms have reached the electronic configuration of Sn atoms long before the Mössbauer γ radiation is emitted. The relevant electronic structure for the interpretation of the Mössbauer spectra is therefore associated with tin.

On the other hand, the position and local lattice environment of the Sn atom may be similar to that of the implanted Sb atom. This would be true, if no atomic diffusion or substantial relaxation occurs within times of the order of the lifetime of the Mössbauer state. It seems unlikely that the intermediate charge state of the Sn atom should cause such motions because the holes are filled in times that are short compared to characteristic lattice vibration times. However, the permanent change in the number of atomic electrons by minus one from the EC decay may cause electronic and geometric relaxations of the surrounding lattice. The characteristic response time of the lattice for such relaxations may be approximated by the dielectric relaxation time ($\epsilon/2\pi\sigma \sim 10^{-12} \times \sigma^{-1}\,\mathrm{s}^{-1}$). For the n-type material used here ($\sim 5\,\Omega$ cm), this relaxation time should be much shorter than the lifetime of the Mössbauer level. Thus the detected signals are from Sn atoms at least with electronic equilibrium. The overall configurational structure, however, could be determined by the Sb atoms, if this structure when associated with a Sn atom, is stable to within the lifetime of the Mössbauer state.

B. Interpretation of ^{119}Sn isomer shifts

The relationship between the isomer shift δ and the electron density at the nucleus $\rho(0)$ is given by the well-known formula[9]

$$\delta = \frac{2\pi e^2 c}{5} \frac{ZR^2}{E_\gamma} \left(\frac{2\delta R}{R} \right) [\rho^e(0) - \rho^a(0)] \ .$$

Here, Z is the nuclear charge, E_γ the energy of the resonant γ quantum, and $\delta R/R$ the relative change of the effective nuclear radius $R = 1.2A^{1/3}$. The quantities $\rho^e(0)$ and $\rho^a(0)$ are the electron probability densities at the nucleus for emitter and absorber, respectively. The calibration constant for this relation for the case of ^{119}Sn is unfortunately not yet determined unambiguously (see Ref. 27). In the following calibration by Antoncik[27] will be used. In particular, the interpretation will be based on an assignment of values of $\delta = 1.3$ mm/s for four electrons in the ideal covalent $5s^1 5p^3$ tetrahedral configuration and of $\delta = 3.2$ mm/s for four electrons in the atomic $5s^2 5p^2$ configuration.

C. Site assignment for line 2

Line 2 ($\delta = 1.83$ mm/s) can be easily identified as due to substitutional Sn atoms since the isomer shift agrees with that found for substitutional ^{119m}Sn in silicon, $\delta = 1.84$ mm/s.[10,12] Also the Debye temperature of this line, $\Theta_2 = 220$ K from temperature-dependent measurements compares well with that found for similar measurements for substitutional ^{119m}Sn, $\Theta = 230$ K.[28] (There is a discrepancy between the f factor at room temperature calculated from the above Debye temperature in a high-temperature Debye approximation and a direct measurement of the f factor at room temperature.[12] This problem will be discussed in the forthcoming paper.[28]) The low linewidth indicates that local disturbances of the surrounding lattice are negligible within the accuracy of Mössbauer spectroscopy.

The isomer shift of the substitutional line 2 is not very close to the value for ideal hybridized covalent bonds. However, from a semiquantitative calculation of the relative isomer shifts for substitutional ^{119}Sn atoms in group-IV elements with diamond structure, the nature of this deviation can be well understood.[12,29,30] It reflects the dehybridization of the $ns\ np^3$ bonds with increasing n. The substitutional ^{119}Sn impurity atoms redistribute their s- and p-valence electrons according to the character of the host bonds, for Sn in silicon an electronic configuration of $5s^{1.6}5p^{2.4}$ is concluded.[12,30]

For samples annealed at $\sim$900 K or implanted at $\sim$750 K,[19] line 2 is found to dominate in all Mössbauer spectra. For such conditions, both Sb and Sn atoms have been determined to be on substitutional sites in silicon by channeling lattice location studies.[10,31,32]

The fact that the Mössbauer results for ^{119m}Sn and ^{119}Sb agree for high-temperature implanted or annealed samples and do give simple lines only indicates that "after effects" are of no importance for substitutional sites.

D. Defect formation by Sb implantations

A comparison of the Mössbauer spectra for room-temperature implantations of ^{119}Sb and ^{119m}Sn can directly determine which lines are related to original Sb defects formed in the silicon lattice and which to original Sn defects. For ^{119m}Sn implantations, only the single-line spectra from substitutional atoms

($\delta = 1.84$ mm/s) have been observed for low doses ($\lesssim 10^{14}$ atoms/cm^2).[10,12] Therefore, the occurrence of line 3 for room-temperature implantations of Sb must be due to different lattice interactions of Sb in comparison with Sn. Since the radiation damage produced in the slowing-down processes is virtually the same for the two ions, the origin of this difference must stem from the difference in the "chemical" interactions of the two elements in the highly reactive surroundings of the disordered regions at the end of the track. Thus, it is tempting to assume that line 3 is due to an Sb daughter defect structure. This structure is either not formed or is thermally unstable at room temperature for times of the order of days in Sn implantations. However, it does not anneal within the lifetime of the Mössbauer state when it is formed after the EC decay of Sb in this structure. The relatively high annealing temperature of the parent defect (between 700 and 900 K) suggests that it is of a more complicated nature than a simple vacancy or interstitial associated with Sb. (For example, the antimony-vacancy pair has been found to anneal below 580 K.[33]) In general, in ion implantations, more complicated defects are produced as compared to irradiations with electrons or neutrons.[4] In accordance with the annealing temperature of the defect, no indication of line 3 has been found for implantations of Sb in silicon at 720 K.[19] Similarly, line 4 has not been observed for annealed samples implanted with Sn.[10,12] Thus, this line is also attributed to an Sb daughter defect structure.

It is interesting to note that in the as-implanted spectra from both samples 1 and 2, a slight indication for some intensity in line 4 can be seen [compare Figs. 1(a) and 1(b)]; however, attempts to include this line in the fit of the spectra did not allow a conclusive decision on the existence of this line in the spectra directly after the implantation.

E. Site assignment for line 3

In this subsection it is shown that the measured Mössbauer parameters and other properties of the line-3 defect are consistent with the identification of this structure as a (nearly) substitutional Sn atom in a multivacancy complex. In a complete discussion, it would be necessary to exclude other lattice positions proposed for heavy impurities, e.g., interstitial sites, or other structural configurations of the defect. However, a detailed discussion of these possibilities is omitted here, since in Part II of this paper, interstitial lattice positions are discussed in connection with the assignment of line 4 to an interstitial position. Furthermore, a new line 1, which is not observed in Sb implantations, is assigned to another possible Sn-vacancy defect of quite different structural configuration. From the discussions of these lines in Part II it emerges clearly that it seems reasonable to exclude a number of other possible structural configurations for the line-3 defect.

Although, as argued before, it seems unlikely that the line-3 defect is a "simple" structure, it is useful to consider the basic effects of the association of one vacancy to a substitutional Sn atom. If a neutral charge state is assumed for the Sn atom, one possible consequence of an adjacent vacancy is that one nominal bond will become a "dangling bond." Compared to substitutional Sn atoms, for this configuration the Debye-Waller factor of the impurity atoms will be drastically lowered, since one of the bond atoms is missing. The effect of a dangling bond on the isomer shift will depend on the rearrangement of the four valence electrons with respect to their p or s character. It seems plausible to assume that the electronic configuration of the valence electrons is changed towards a higher s-like character, since the strength of the directional hybridized bonds is correlated with the p character of the bonds.[12] From the lack of cubic symmetry for a vacancy associated substitutional Sn site, a quadrupole splitting of the Mössbauer line is expected due to the occurrence of an electric field gradient at the Sn site. Qualitatively, the effects sketched above are all observed for the line-3 defect, if the line broadening is attributed to an unresolved quadrupole splitting.

The above model of a substitutional Sn impurity atom with a dangling bond towards an adjacent vacancy is structurally similar to the model proposed by Elkin and Watkins[34] from ESR studies for the Sb-vacancy pair. For the zero-charge ground state of this structure, a Jahn-Teller distortion was concluded in which two of the three silicon atoms adjacent to the vacancy pull together to form an electron pair bond. About 60% of the wave function of the paramagnetic electron was concluded to be located in a dangling bond on the third silicon atom. Only 4% of the wave function was attributed to a dangling bond on the Sb impurity atom. From γ and e^- irradiations, Sb atoms are known to be efficient vacancy traps in silicon.[33,34] Therefore, the occurrence of vacancy associated Sb atoms is to be expected also for Sb^+ ion implantations. The high concentration of primary defects in the vicinity of the implanted Sb atoms makes the formation of multivacancy defects much more likely for this case than for γ or e^- irradiations. Thus, the observation of a Sn daughter defect with a configuration which is structurally similar to that of the Sb-vacancy pair seems reasonable, if the Sb multivacancy parent defect is related to the Sb-vacancy pair and if no strong relaxation of the structure occurs within the lifetime of the Mössbauer state.

On the other hand, a strong relaxation after the nuclear decay of Sb to Sn would be plausible, since quite a different structural and electronic configuration than for the Sb-vacancy pair has been proposed

for the Sn-vacancy pair.[35] In this defect the Sn atom is located on an interstitial site in the center of a divacancylike defect with six bonds to its nearest neighbors. Without going into a detailed discussion here, it can be said that it seems to be excluded that the line-3 defect shows any similarity with this structure. In Part II of this paper, a detailed argumentation is given for the assignment of another defect line 1 observed in ^{119}Sn Mössbauer spectra from ^{119m}Te implantations to this Sn-vacancy structure. Thus, there is no indication from the present experiment of a large displacement of the Sn atoms from a substitutional site in the Sb-daughter defect. This (nearly) substitutional site of the Sn atoms is probably inherited from the Sb mother defect structure. A nearly substitutional site of the Sb atoms in a multivacancy defect structure would be in accordance with the annealing behavior of line 3, since the Sb atoms are located on substitutional sites after the annealing.

Although large displacements of the Sn atoms from the substitutional site in the line-3 defect seem to be excluded, it seems unlikely that no relaxation should occur, since the Sb-vacancy pair shows considerable lattice relaxation,[34] and the probability for relaxations should be even higher for a Sb multivacancy complex. Therefore, the possibility of lattice relaxations of the Sn atoms or the silicon atoms adjacent to the vacancies has to be taken into account in a more realistic model of the line-3 defect. As long as these relaxations result in a slight displacement from the substitutional site, it seems likely that the electronic configuration of the Sn atoms is hardly affected, whereas the vibrational modes might be much more sensitive to such lattice distortions.

Alternatively to a dangling bond for the substitutional Sn atom in the line-3 defect, the formation of an "extended bond" to Si neighbor atoms adjacent to the vacancy seems possible. Such bonds have been proposed to be formed by another group-IV impurity atom, germanium, in a Ge-vacancy pair, where the Ge atoms are located on substitutional sites.[36] Since these bonds are likely to be weak compared to the remaining three hybridizing bonds, their influence on the lattice position and the Debye-Waller factor may be small, whereas the electronic configuration of the Sn atoms might be rather different from the case of a dangling bond.

From the qualitative discussion given above, it emerges that the experimental evidence on the line-3 defect is consistent with a model of a (nearly) substitutional Sn atom associated with more than one vacancy. The Sn atom may have a dangling bond or some weak extended bond to Si atoms adjacent to a neighboring vacancy. Also a relaxation of the defect structure, resulting in a slight displacement of the Sn atoms from a substitutional site seems likely.

In the following an attempt is made to estimate the effect of a single dangling bond on the Mössbauer parameters of a substitutional Sn atom in order to arrive at a somewhat more quantitative model for the line-3 defect structure. From this estimate, some insight into the importance of geometrical and electronic relaxations is obtained.

The isomer shift change due to a dangling bond will be approximated by proportional changes in the electron density due to changes of the valence electron character from p to s character. In this approach, any influence of the d electrons and the screening of the s by the p or s electrons is neglected; both assumptions seem to be reasonable in this context.[27,30] In this approximation the electronic configuration of an ideally tetrahedrally bonded Sn atom (with an isomer shift of $\delta = 1.3$ mm/s) is $5s^1 5p^3$ and that of an atomic configuration of an unbound atom $5s^2 5p^2$ (with an isomer shift of $\delta = 3.2$ mm/s). Suppose the effect of one dangling bond can be estimated by a linear interpolation between the above two configurations, then the effect on the isomer shift should be an increase by $\sim\frac{1}{4}(3.2-1.3)$ mm/s ~ 0.5 mm/s. Taking into account that the isomer shift of substitutional Sn in silicon indicates a considerable dehybridization as compared to ideal covalent bonds, the estimated value would be less. On the other hand, a geometric relaxation from the substitutional site and/or an electronic relaxation of the remaining three bonds will probably lead to a further dehybridization, i.e., an increase in isomer shift. Thus the observed relatively large increase of the isomer shift by ~ 0.8 mm/s for the line-3 defect as compared to a substitutional site suggests that at least electronic relaxations are of importance for a realistic model of the defect.

From the noncubic symmetry of a vacancy associated substitutional Sn atom, a quadrupole splitting (or broadening) of the line is expected. Since the electric field gradient at the Sn nucleus will be predominantly determined by the unbalanced p electrons, the quadrupole splitting may be estimated from the increase in isomer shift by using an empirical relation between the isomer shift and the quadrupole splitting for tin II compounds.[37] From this the expected quadrupole splitting is estimated to ~ 0.4 mm/s, in reasonable agreement with the experimental line broadening of ~ 0.3 mm/s.

For a discussion of the measured Debye-Waller factors, the Debye model will be used. In this model, for a monoatomic crystal lattice bound in harmonic forces, the force constant between neighboring atoms is given by $\gamma = (\text{const})\Theta^2 M$, where Θ is the Debye temperature of the material and M is the mass of the atoms.[9] If an impurity of mass M' is introduced substitutionally into the lattice, the effect of the mass difference between the impurity and the host atoms can be accounted for by an effective characteristic temperature for the impurity atom given by $\Theta_{\text{eff}} = \Theta(M/M')^{1/2}$.[38] Using a value of

$\Theta = 543$ K for silicon,[39] we find $\Theta_{\text{eff}} = 260$ K for substitutional tin atoms, in rough agreement with the value of $\Theta_2 = 220(20)$ K as extracted from the measurements at 77 and 297 K.

For a discussion of the Debye temperature obtained for the site 3 the effect of a dangling bond on the impurity atom may be estimated by assuming that the force constant in a Debye model is lowered by about a factor $d = \frac{3}{4}$ for one broken bond. We then find an effective Debye temperature for such a defect structure by $\Theta^d_{\text{eff}} = \Theta(M/M')\sqrt{d}$. We calculate $\Theta^d_{\text{eff}} = 190$ K (using the experimental Debye temperature of line 2). This value is to be compared with a measured value of $\Theta = 160$ K. The considerably lower experimental value (which, in the framework of this simple model would be in agreement with two broken bonds for the impurity atoms) indicates the possibility of relatively large geometrical relaxations.

In summary, our model is oversimplified. On the other hand, both the low Debye temperature and the enhanced s character deduced for the valence electrons of the impurity atoms from the isomer shift, are in accordance with each other since a weakening of the hybridized bonds in group-IV semiconductors is correlated with an enhanced s character of the valence electrons.[12,40] Such a weakening may occur for a relaxation of the impurity atom in the direction of one adjacent vacancy, so that both the measured isomer shift and the Debye temperature for this line are not in contradiction with the assumption of one dangling bond for the Sn atoms. If it is assumed from the experimental Debye temperatures that the vibrational amplitudes of the impurity atoms increase considerably only in the direction of the vacancy, then the mean-squared vibrational amplitude is calculated to be four times larger in this direction than for a regular substitutional impurity atom.

It is interesting to note that whereas no obvious connection seems to exist to the ^{119m}Sn defect structures found in neutron irradiation,[14] the Mössbauer spectrum observed after the thermal-neutron capture process $^{118}\text{Sn}(n,\gamma)^{119m}\text{Sn}$ for Sn in silicon does show two lines (of about equal intensity) with isomer shifts very close to those of lines 2 and 3 [$\delta \approx 1.8$ and 2.7 mm/s (Ref. 15)]. However, these lines are interpreted by Nistiryuk and Seregin as a quadrupole doublet due to Sn in an interstitial position with an associated vacancy.[15] It is not evident from their argumentation whether an interpretation in terms of two independent lines is excluded.

F. Site assignment for line 4

A detailed discussion of the parameters of line 4 will be given in Part II of this paper on implantations of ^{119m}Te in silicon. New aspects on the character of this line emerge from those experiments. Here, the conclusions given in Part II will be anticipated: line 4 is due to interstitial impurity atoms having approximately the atomic $5s^25p^2$ configuration. The isomer shift of $\delta = 3.3$ mm/s is slightly higher than measured for interstitial atoms in a rare-gas matrix, $\delta = 3.2$ mm/s,[41] the difference is attributed to a compression of the large impurity atoms. It should be noted that the isomer shift and the Debye temperature of line 4 are well determined from the Sb implantations reported here.

G. Annealing experiments

Annealing experiments reveal details about the thermal properties of Sb defect structures since the annealing is over before the Sb decays. From the two series of annealing experiments on the implanted samples, the annealing temperature for the line 3 defect is determined to be between 700 and 900 K. This temperature range has been found to be typical for the annealing of complicated defect agglomerates in ion implanted silicon.[4] Disordered regions or even amorphous layers produced by ion implantation are known to anneal at about 900 K. For the low implantation dose of the second sample in Table I ($\lesssim 10^{13}$ atoms/cm^2), the formation of an amorphous layer is unlikely, since the amorphisation dose has been determined to be $\gtrsim 10^{13}$ atom/cm^2.[42] Thus the defect structures should be those formed in the damage cascades at the end of the track. Some annealing or agglomeration of these defect structures is expected, since several simple defects are known to be unstable or mobile at room temperature. A reordering of the lattice disorder introduced by 200-keV Sb ions in silicon was observed below room temperature in channeling studies.[43] The implanted dose for the first sample of Table I ($\approx 10^{14}$ atoms/cm^2) is above the amorphous dose. However, no pronounced differences in the Mössbauer spectra of the two samples are observed.

The increase of line 4 after the different annealing steps is attributed to a trapping of the impurity atoms in interstitial sites, probably in agglomerates with a number of silicon interstitials. Extended agglomerates of impurity atoms and self-interstitials are proposed as a high-temperature defect structure in high-purity silicon.[44] Alternatively, the growing in of line 4 might be due to precipitation. This seems less likely, however, since the concentration in the implanted layer does not exceed the solid solubility of Sb in silicon.

H. Site assignment for line 3′

The occurrence of the line at $\delta = 2.6$ mm/s after the annealing at ~ 1400 K is possibly due to Sb atoms which migrate, get trapped, and end up decorating

the residual extended damage structures in the implanted layer. Such structures are known to remain in Sb-implanted silicon layers even after high-temperature annealing.[45] By removing about 200 Å from the surface of the sample in an etching procedure with HNO_3 and HF, it was proved that Mössbauer signals from both lines 3′ and 4 do originate from the implanted layer even after the high-temperature annealing. The resulting spectrum from the etched sample (see Table I) only showed the substitutional line, which originates from Sb partly diffused into the unimplanted bulk material. (After a 20-min annealing at ~1200 K, it is known that a considerable fraction of the implanted Sb atoms diffuse out of the implanted layer.[46])

From the constancy of the sum of defects in the annealing steps up to ~1400 K, no change in f factor for the lines 2 and 4 is indicated. However, there is a drastic change of the f factor between lines 3 and 3′ after the 1400 K annealing, in accordance with the Debye temperatures determined from the temperature dependence of the f factors. This result indicates that, although the electronic structures of the impurity atoms in the defects assigned to lines 3 and 3′ (i.e., implanted and after an annealing at ~1400 K) are apparently similar, their local surrounding or possibly their coupling to the host lattice must be distinctly different. If the impurity defect structure is considered a "molecule" in the host lattice, the electronic structure of the impurity atom will be predominantly determined by their "molecular" bonds. The f factor, however, will be sensitive not only to intramolecular vibrational modes, but also to the coupling of the "molecule" to the host lattice. This coupling is expected to be different for different defects. The measured isomer shift possibly indicates that line 3′ may be due to Sn atoms in an extended vacancy structure.

1. Comparison with channeling experiments

The above results imply that an increasing fraction of Sb atoms occupy nonsubstitutional sites in the silicon lattice when the samples are annealed at higher temperatures (900–1200 K). No indication for such fractions have been found in channeling studies for the lattice location of Sb in silicon[31,32] and, in particular, no measurable fraction was found in the interstitial holes along the ⟨111⟩ axial direction. However, Davies *et al.*[47] observed a drastic decrease of the substitutional fraction (to ~40%) after an annealing at 1170 K. This was attributed to an outdiffusion of a large fraction of the implanted atoms because the removal of ~50 Å from the implanted layer caused an increase of the substitutional fraction to ~90%. Therefore, the question arises whether line 4 and line 3′ might be due to Sb atoms in the SiO_2/Si interface. This seems to be excluded, however, since a removal of the SiO_4 layer by an HF treatment after an annealing at ~900 K did not change the intensity of line 4. Furthermore, in Part II of this paper, evidence for an annealing of both lines is found, which is unlikely to occur for atoms trapped at the SiO_2 surface layer.

Recently, Swanson *et al.*[48] by channeling experiments measured an irradiation (He^+, 2 MeV) induced displacement of substitutional Sb diffused into silicon. This displacement of the order of 0.2–0.6 Å was attributed to the trapping of several vacancies at the impurity atoms. The authors also suggested that a narrowing of channeling dips observed for implanted Sb^{32} might be due to similar defects. This vacancy cluster model agrees well with the model proposed for the line 3 defect in this investigation. In particular, a displacement of the Sb atoms from a substitutional position towards an adjacent vacancy is supportive as discussed in Sec. IV E for the relatively high isomer shift and low Debye temperature of line 3. On the other hand, it seems not excluded, that large vibrational amplitudes of the Sb impurity atoms in the direction of the vacancy can account for a substantial part of the apparent displacements as seen by channeling experiments.

V. CONCLUSION

Mössbauer emission spectra from ^{119}Sn atoms whose parent was implanted radioactive ^{119}Sb in silicon have been interpreted in terms of four independent lines. These lines are characterized primarily by their isomer shifts and Debye temperatures. The four line interpretation was determined from the observed annealing properties and temperature dependences of the line intensities. The strongest line is identified to be due to substitutional Sn atoms in a locally undisturbed surrounding. A second line is attributed to Sn atoms on (nearly) substitutional sites associated with vacancies. A third line with the same isomer shift as the foregoing is interpreted as stemming from impurity atom in an extended vacancy complex formed at high temperatures. The fourth line is attributed to a minor fraction ($\lesssim$10%) of impurity atoms in interstitial sites.

The vacancy associated defect structure is found to anneal between 700 and 900 K. The electronic configuration of the Sn impurity atoms in this defect structure is characterized by an increased fraction of s electrons compared to a substitutional site. This is attributed primarily to a dangling bond into adjacent vacancies, causing a redistribution of the valence electrons from an sp^3 hybrid character towards an atomic s^2p^2 configuration. Secondarily, the defect structure may be relaxed, causing a slight displacement of the Sn atoms from substitutional sites. The observed line broadening is in accordance with the above electronic redistribution attributed to a quadru-

pole splitting. The reduction of the Debye-Waller factor for this defect structure compared to a substitutional site is in qualitative agreement with the above model assignment.

After high-temperature ($\gtrsim$1200 K) annealings, impurity atoms are found in an electronically similar configuration but with a considerably higher Debye-Waller factor in a defect attributed to Sn atoms which decorate extended residual damage structures (possibly vacancy loops).

At the higher annealing temperature, an increasing fraction of impurity atoms occupy interstitial sites, probably in agglomerates with silicon self-interstitials. For the Sn atoms in these sites, the isomer shift is attributed to an electron density characteristic of an atomic s^2p^2 configuration and compressional effects due to the volume excess of the impurities. The Debye-Waller factor in these sites is found to be larger than that for substitutional sites.

The complex defect structures found besides undisturbed substitutional sites for the ^{119}Sn atoms after implantations of $^{119}Sb^+$ ions are related to the implantation behavior of the Sb^+ ions since no such defects are found for ^{119m}Sn implantations.

---

*Present address: Central Bureau of Nuclear Measurements, Geel, Belgium.

[1]S. Namba, *Ion Implantation in Semiconductors* (Plenum, New York, 1975).

[2]F. Chernow, J. A. Borders, and D. K. Brice, *Ion Implantation in Semiconductors* (Plenum, New York, 1977).

[3]J. Bourgin, in Ref. 1, p. 385.

[4]J. W. Meyer, L. Eriksson, and J. A. Davies, *Ion Implantation in Semiconductors* (Academic, New York, 1970).

[5]D. K. Brice, in Ref. 1, p. 399.

[6]E. Bøgh, P. Høgild, and I. Stensgaard, in Proceedings of the IAEA Symposium on Radiation Damage in Reactor Materials, Vienna, 1969, p. 77; Radiat. Eff. 7, 115 (1971).

[7]D. A. Thompson, R. S. Walker, and J. A. Davies, Radiat. Eff. 32, 135 (1977).

[8]L. C. Kimerling and J. M. Poate, in *Proceedings of the International Conference on Lattice Defects in Semiconductors, Freiburg, 1974*, edited by F. A. Huntley (Institute of Physics, Bristol, 1975), p. 126.

[9]V. I. Goldanskii and R. H. Herber, *Chemical Applications of Mössbauer Spectroscopy* (Academic, New York, 1968).

[10]G. Weyer, J. U. Andersen, B. I. Deutch, J. A. Golovchenko, and A. Nylandsted Larsen, Radiat. Eff. 24, 117 (1975).

[11]I. V. Nistiryuk and P. P. Seregin, Sov. Phys. Solid State 17, 768 (1975).

[12]G. Weyer, A. Nylandsted Larsen, B. I. Deutch, J. U. Andersen, and E. Antoncik, Hyper. Inter. 1, 93 (1975).

[13]P. P. Seregin, I. V. Nistiryuk, and F. S. Nasredinov, Sov. Phys. Solid State 17, 1540 (1975).

[14]K. Matsui, R. R. Hasiguti, T. Shoji, and A. Ahkawa, in *Proceedings of the International Conference on Defects in Semiconductors, Freiburg, 1974*, edited by F. A. Huntley (Institute of Physics, Bristol, 1975), p. 572.

[15]I. V. Nistiryuk and P. P. Seregin, Sov. Phys. Solid State 18, 673 (1976).

[16]J. R. Teague, C. M. Yagnik, G. J. Long, and R. Gerson, Solid State Commun. 9, 1695 (1971).

[17]M. van Rossum, J. de Bruyn, G. Langouche, R. Coussement, and P. Boolchand, J. Phys. (Paris) 37, C6-889 (1976).

[18]A. Nylandsted Larsen, G. Weyer, B. I. Deutch, E. Antoncik, and H. Loft Nielsen, J. Phys. (Paris) 37, C6-883 (1976).

[19]G. Weyer, A. Nylandsted Larsen, B. I. Deutch, E. Antoncik, and H. Loft Nielsen, in *Proceedings of the International Conference on Radiation Effects in Semiconductors, Dubrovnik, 1977*, edited by N. B. Urli and J. W. Corbett (Institute of Physics, Bristol, 1977), p. 491.

[20]Y. Llabador, J. Inorg. Chem. 36, 2453 (1974).

[21]F. Ambe and S. Ambe, J. Phys. (Paris) 37, C6-923 (1976).

[22]G. Weyer, Mössbauer Eff. Methodology 10, 301 (1976).

[23]D. W. Palmer, in *Proceedings of the International Conference on Radiation Effects in Semiconductors, Dubrovnik, 1977*, edited by N. B. Urli and J. W. Corbett (Institute of Physics, Bristol, 1977), p. 144.

[24]R. L. Kauffmann, C. W. Woods, K. A. Jamison, and P. Richard, Phys. Rev. A 11, 872 (1975).

[25]W. Bambynek, B. Crasemann, R. W. Fink, H. M. Freund, H. Mark, C. D. Swift, and P. Venngopala Rao, Rev. Mod. Phys. 44, 716 (1972).

[26]R. L. Kaufman, K. A. Jamison, T. C. Gray, and P. Richard, Phys. Rev. Lett. 36, 1074 (1976).

[27]E. Antoncik, Phys. Status Solidi B 79, 605 (1977).

[28]J. W. Petersen, O. H. Nielsen, G. Weyer, S. Damgaard, and E. Antoncik, Phys. Rev. B (to be published).

[29]E. Antoncik, in *Proceedings of the International Conference on Lattice Defects, Frieburg, 1974*, edited by F. A. Huntley (Institute of Physics, Bristol, 1975), p. 565.

[30]E. Antoncik, Hyper. Inter. 1, 329 (1976).

[31]L. Eriksson, J. A. Davies, N. G. E. Johannson, and J. W. Mayer, J. Appl. Phys. 40, 842 (1969).

[32]D. Sigurd and K. Björkqvist, Radiat. Eff. 17, 209 (1973).

[33]M. Hirata, M. Hirata, and H. Saito, J. Phys. Soc. Jpn. 27, 405 (1969).

[34]E. L. Elkin and G. D. Watkins, Phys. Rev. 174, 881 (1968).

[35]G. D. Watkins, Phys. Rev. B 12, 4383 (1975).

[36]G. D. Watkins, IEEE Trans. Nucl. Sci. 16 - 6, 13 (1969).

[37]J. K. Lees and P. A. Flinn, Phys. Rev. 48, 882 (1968).

[38]Y. Kagan and Y. A. Iosilevskii, Sov. Phys. JETP 15, 182 (1962).

[39]B. W. Batterman and D. R. Chipman, Phys. Rev. 127, 690 (1972).

[40]A. Nylandsted Larsen and G. Weyer, J. Phys. F 9, 27 (1979).

[41]H. Micklitz and P. H. Barrett, Phys. Rev. B 5, 1704 (1972)

[42]E. C. Baranova, J. U. Gusev, Yu. V. Martynenko, C. V. Starinin, and I. B. Hailbullin, in *Ion Implantation in Semiconductors*, edited by I. Ruge and J. Gaul (Springer, Berlin, 1973), p. 59.

[43]S. T. Picraux, W. H. Wisenberger, and V. L. Vook, Radiat. Eff. 7, 101 (1971).

[44]A. Seeger, H. Föll, and W. Frank, in *Proceedings of the International Conference on Radiation Effects in Semiconductors, Dubrovnik, 1977*, edited by N. B. Urli and J. W. Corbett (Institute of Physics, Bristol, 1977), p. 12.
[45]S. M. Davidson and G. R. Booker, Radiat. Eff. 6, 33 (1970).
[46]S. Namba, K. Masuda, K. Gamo, A. Doi, S. Shinji, and T. Kimura, Radiat. Eff. 6, 115 (1970).
[47]J. A. Davies, J. Denhartog, L. Eriksson, and J. W. Mayer, Can. J. Phys. 45, 4053 (1967).
[48]M. L. Swanson, J. A. Davies, A. F. Quenneville, F. W. Saris, and L. W. Wiggers, Radiat. Eff. 35, 51 (1978).